Materials Research. 2018; 21(1): e20170641
DOI: http://dx.doi.org/10.1590/1980-5373-MR-2017-0641

Conducting Behavior of Crystalline α-PbO_2 as Revealed by DFT Calculations

***João Manuel Marques Cordeiro*[a]*, Douglas Henrique Marcelino de Azevedo*[a], *Tatiana Conceição Machado Barretto*[a], *Julio Ricardo Sambrano*[b]**

[a]*Faculdade de Ciências Naturais e Engenharia, Universidade Estadual Paulista - UNESP, 15385-000, Ilha Solteira, SP, Brazil*
[b]*Grupo de Modelagem e Simulação Molecular, Universidade Estadual Paulista - UNESP, 17033-360, Bauru, SP, Brazil*

Received: July 11, 2017; Revised: October 30, 2017; Accepted: November 10, 2017

PbO_2 is one material that has recently emerged as potential transparent conducting oxide for applications in the modern opto-electronic industry. In this work the electronic structure of the α-PbO_2 polymorph has been investigated, aiming to contribute to the understanding of its high levels of conductivity. DFT calculations using B3LYP hybrid density functional and considering long range interactions among the atoms have been performed. A direct band gap of 0.90 eV has been found, compatible with high conductivity values. Although the stoichiometric material is somewhat transparent, the band structure indicates that appropriated modifications in the material Fermi level can be performed in order to decrease the absorption of light. Charge distribution plus overlap population analysis show that the material is predominantly ionic. The charge distribution throughout the material is strongly dependent on the crystal direction. Results suggest that α-PbO_2 can be potentially more interesting for opto-electronic purposes than the β polymorph.

Keywords: *Lead dioxide, transparent conducting oxides, density functional theory, optical band gap*

1. Introduction

The modern optoelectronic technology is highly dependent on transparent conducting oxides (TCOs), compounds which combine transparency and conductivity, properties that normally do not coexist. Initially that technology was mainly based on In_2O_3, a rather expensive material due to the scarcity of indium in the earth (In is obtained as a by-product of refining other metals like Zn and Pb, for example, and the amount of In available in the minerals is not known). Because of that it has been intensely sought alternative materials to replace it.[1] SnO_2 and ZnO are among the materials that have proved to be quite competitive as substituents to In_2O_3. Low coast and recent progress in improving performance make them attractive substitutes for the indium based TCOs.[2] However, the investigation has not over and new materials are insistently sought after. Among the new investigated materials, PbO_2 arises as a very promising one, which electrical properties have been explored very recently.[3-8] PbO_2 has a high chemical stability and because of the lower coast of Pb compared to In, achieving optical transparency with high electrical conductivity could have important reflexes in optoelectronic industry in the medium-term. Even though Pb is not environmentally friendly, it is highly likely that the economic benefits outweigh the expense of the logistics involved in recycling. Above all, it is highly significant, from a social point of view, finding new and cheaper materials that can guarantee to countries with lower purchasing power access to the most modern technologies.

An orthorhombic (columbite) α, a tetragonal (rutile) β, and a high-pressure γ modification polymorphs of PbO_2 have been identified. Both the α-phase (space group Pbcn), and β-phase (space group P42/mnm) are stable under normal conditions, the β-phase being the most stable in acid medium and the α-PbO_2 prevailing in neutral/alkaline solutions.[9] The active material of positive plate of the lead-acid batteries is a mixture of α- and β-PbO_2.[10]

Most of the TCO's are n-type semiconductors having a band gap of the order of ~3 eV, optical transmittance in the visible region higher than 80%, and electrical resistance less than or equal to 10-3 Ω.cm.[11] From the carried out studies reported up to now is very well established that β-PbO_2 is intrinsically metallic or a narrow band gap (NB) semiconductor,[6-8] with a band gap of 0.61 eV, and a carrier concentration about 10^{21} cm^{-1}.[12] NB semiconductors are colored or black when closed to stoichiometry, which is the case of β-PbO_2, but may potentially become transparent when donor doped to high carrier concentrations, as it has been found for CdO,[13,14] thanks to the blue-shift of the optical band gap, following the Moss-Burstein effect.[15,16] The shift arises because the Fermi energy lies in the conduction band for heavy n-type doping and, consequently, the filled states block optical excitation. Thus, the band gap determined from the onset of interband absorption moves to higher energy.

*e-mail: cordeiro@dfq.feis.unesp.br

However, achieving optical transparency also depends on the conduction band structure. The optical transparency is guaranteed since the transitions from the filled conduction band states to the next highest conduction band lie above the threshold for visible light absorption.[17,18]

β-PbO_2 typically displays degenerate n-type conductivity attributed to oxygen vacancies. The oxygen stoichiometry is critical to the conductivity, since each lack of oxygen contribute with two free electrons. The calculated Fermi energy lies deep in the conduction band, which is consistent with high levels of electrical conductivity.[8]

However, if on one hand, there are still many gaps to be filled concerning to the electronic properties of β-PbO_2, on the other hand no study was found in the literature related to those properties of α-PbO_2. In this paper are being reported the first results related to a systematic investigation on the α-PbO_2 electronic properties, as revealed by calculations based in density functional theory (DFT), aiming to evaluate its potential to be applied as TCO.

2. Model and Computational Method

As already stated in the introduction, α-PbO_2 has an orthorhombic symmetry with 4 formula units per unit cell. Neighbor unit cells share non-opposing edges, resulting in the formation of zigzag chains, according to Figure 1. The material consists of Pb or O interleaved planes in the direction [001] and a sequence of PbO_2 planes in the direction [111] with Pb atoms hexa-coordinated and O atoms tetra-coordinated. The computational simulations were performed in the framework of the periodic DFT implemented in the crystalline orbital computer code CRYSTAL14.[19] DFT is a powerful methodology to simulate structural, energetic and electronic properties of solid state materials with high accuracy, thanks to the advent of functionals based on the generalized gradient approximation.[20,21] A deep analysis on the reproducibility of DFT calculations of solids has been published recently.[22,23] Crystalline orbitals were represented as a linear combination of Bloch functions defined in terms of local functions (atomic orbitals) using Gaussian-type basis set.[24]

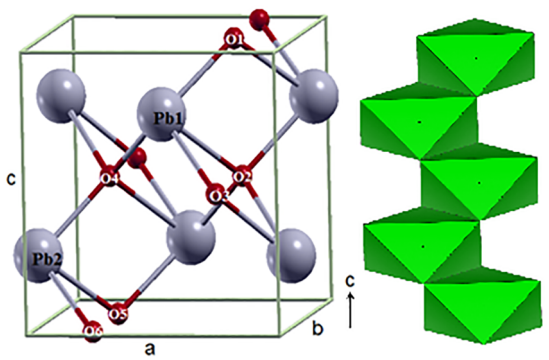

Figure 1. The unit cell and zigzag chain of α-PbO_2 (some atom labels are numbered for later discussion).

Taking into account that the choice of the proper functional is fundamental for the quality of the results, two of them have been tried for us: the B3LYP,[25,26] and the HSE06[27] ones. B3LYP is a very popular functional used with DFT for studying solids. It is a type of approximation to the exchange-correlation energy, based in the scheme introduced by Axel Becke in 1993.[25] A comprehensive analysis of the performance of B3LYP functional for a broad set of molecules has been reported by Jorgensen and Tirado-Rives.[28]

On the other hand, HSE06 is a functional derived from the PBE one,[29-31] that apply a screened Coulomb potential to the exchange interaction in order to screen the long-range part of the Hartree-Fock exchange.[27] This functional was implemented into CRYSTAL in the 2014 version. When using the B3LYP functional the long range interactions were considered by adopting the Grimme approach[32,33] (in this case the functional is named B3LYP-D).[34] In this approaching the DFT total energy is augmented with a semi-empirical dispersion term based on an additive atom-atom damped empirical potential, according to:[34]

$$E_{disp} = -s_6 \sum_{i=1}^{N_{at}-1} \sum_{j=i+1}^{N_{at}} \sum_{g} \frac{c_6^{ij}}{R_{ij,g}^6} f_{dmp}(R_{ij,g}) \qquad (1)$$

where the summation is over all atom pairs and **g** lattice vectors excluding the $i = j$ contribution for $\mathbf{g} = 0$, s_6 is a scaling factor related to the functional used, c_6^{ij} is the dispersion coefficient for the pair ij computed by using a geometric mean and $R_{ij,g}$ is the interatomic distance between atoms i in the reference cell and j in the neighboring cells at distance ||g||. The dumping function f_{dmp} is used to avoid singularities for small $R_{ij,g}$ distances. Such function is implemented in the CRYSTAL14 package as:[34]

$$f_{dmp}(R_{ij,g}) = \frac{1}{1 + e^{-d(R_{ij,g}/R_{vdW} - 1)}} \qquad (2)$$

were d is the constant that determines the steepness of the dumping function, and R_{vdW} is the sum of van der Waals atomic radii for atom pair ij. For the calculations the dispersion term used was $s_6 = 1.05$ (concerning to the B3LYP hybrid functional) and the steepness of the dumping function d = 20. Quite recently a new routine has been implemented for Grimme (named D3), where the atomic radius of each atom is adjusted accordingly to the chemical surroundings and the atomic coordination number.[20,21] This methodology has not been used in the present simulations, since it is not implemented in the commercial version of CRYSTAL14, but may be applied in the future, which may lead to better results. A cutoff radio of 25.0 Å was used to truncate the summation over the lattice vectors.[35] The R_{vdW} and c_6^{ij} parameters used for Pb were those optimized for PbO by Canepa et al.[36] Although these parameters have not been specifically optimized for α-PbO_2 and so do not account exactly its chemical environment, they improved the description of the α-PbO_2 properties compared to not

consider dispersion factor. The C_6 and R_{vdW} parameters used for Pb were, respectively, 63.16 and 1.767,[36] and for O were 0.70 and 1.342.[33]

A full optimization procedure was carried out to determine the equilibrium geometry. All structures were optimized by the use of analytical energy gradients with respect to atomic coordinates and unit cell parameters. Convergence was checked on gradient components and nuclear displacements with tolerances on their root mean square set to 0.0001 and 0.0009 a.u., respectively. The level of accuracy of the calculation of Coulomb and the exchange series is controlled by five parameters. The 8, 8, 8, 8, and 14 parameters were chosen for the Coulomb overlap, Coulomb penetration, exchange overlap, first exchange pseudo-overlap, and second exchange pseudo-overlap, respectively. The shrinking (Monkhorst-Pack and Gilat)[37] was set up to 6, which corresponds to 40 independent k-points in the irreducible part of the Brillouin zone integration.

Mulliken population analysis was used. This choice was based on the simplicity, frequent application in theoretical calculations of similar systems, and convenient interpretation of the results on the light of chemical intuition. The XCrysDen program was used to draw the draft of the band structure, density of states (DOS) graphics, and maps of charge density distribution.[38]

Since the choice of the optimal basis set is difficult for such crystalline materials, several of them have been tested to simulate the material. Two all-electron basis sets have been tried for oxygen: a 6-31G* basis set optimized by Gatti et al.[39] and the Triple Zetta Plus Polarization (TZVP) reported by Peintinger et al.[40] In turn Pb was described for an effective core pseudopotential DB31G* (where DB stands for Durand-Barthelat's large effective core potential),[41] the HAYWLC-211(1d)G,[42] and the ECP60MDF-6111(51d)G.[43] Pb was treated in the framework of core pseudopotential approximation, because its number of electrons makes the simulations very expensive. The lattice parameters reported by Scanlon et al.[4] were fitted to decide on the better computational conditions for the simulations. To the best of our knowledge these are the only experimental properties that have been published for the material. Even the value of the band gap, which would be extremely useful to judge about the quality of results, is unknown. The analysis of the results permits to conclude that the B3LYP-D functional with oxygen 6-31G* and the DB31G* pseudopotential for lead were the computational conditions which provided the best agreement between the theoretical and experimental crystalline structure and were used for calculation of the reported results. Just to give an idea of the divergence, results obtained for α-PbO_2 with B3LYP and HSE06 functionals using those basis set are shown in the Table 1.

3. Results and Discussion

The experimental lattice parameters for α-PbO_2, have been recently obtained using neutron diffraction at ISIS Spallation Neutron Source - Rutherford-Appleton Laboratory (UK),[4] facility which has also been used for us to investigate the structure of other systems.[44-47]Table 1 shows the set of cell parameters of experimental and calculated results obtained for the oxide.

As it can be noticed from the Table, the parameters calculated with B3LYP-D functional show a better agreement with the experimental data available than the results obtained with HSE06 one, which determined the choose of the first functional to perform the simulations. This functional has been very successful in describing electronic and structural properties of several oxides and other materials.[34,48-50] It deserves to point out that calculations without considering long range weak interactions give cell parameters in better agreement with the experimental ones (calculations were performed using the same input script excepting the GRIMME calculation routine). However, it was opted for keeping this routine in the simulations since describing better the interactions between the atoms must reflect in a better quality of the calculated electronic properties (also the comparison with HSE06 functional is more appropriated, since this functional considers long range weak interactions in its formalism).

The band structure of α-PbO_2 obtained from the calculations is shown in Figure 2. Both the top of valence band and the bottom of the conduction band are situated on the same Γ point, resulting in a direct band gap of 0.90 eV. It is worth remembering that pure density functionals like GGA and LDA usually underestimate band gaps, while hybrid functionals, as the B3LYP used in this work, usually provide a good agreement with experimental values.[34,48-50] However, calculations performed in parallel for β-PbO_2 using both B3LYP and HSE06 functionals gave a band gap value of 0.21 eV, while the experimental value is 0.61 eV.[4] Thus, both the functionals tried for us underestimated the β-PbO_2 band gap for about 66% respecting to the experimental value.

Table 1. Experimental[4] and calculated (oxygen 6-31G* and lead DB31G*) equilibrium lattice parameters and density for α-PbO_2. Percentage deviation (%) in parenthesis.

	a (Å)	b (Å)	c (Å)	d(g.cm^{-3})
Experimental	5.001	5.931	5.443	9.820
B3LYP	5.100(2.00)	5.931(0.00)	5.393(0.92)	9.939(1.21)
HSE06	5.224(4.48)	5.517(6.98)	5.259(3.38)	10.624(8.19)

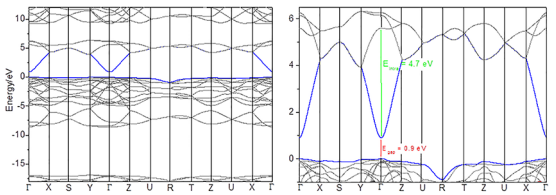

Figure 2. Band structure of α-PbO_2, with the energy scale set so that the Fermi level corresponds to 0.0 eV. (left and right graphics differ in the plotted energy range).

Taking into account this result it can be considered that the α-PbO_2 band gap is at least 0.90 eV. In other words, can be inferred that the α-PbO_2 is less metallic than β-PbO_2, which is a sufficient reason to suppose that α-PbO_2 would be a better candidate for TCO than β-PbO_2. Interestingly, it has been reported that β-PbO_2 (plattnerite) is black and opaque, while α-PbO_2 (scrutinyite) is brown and somewhat transparent.[51]

The topography of the α-PbO_2 band structure on the Γ point is very similar to that of β-PbO_2, however, while in the β-PbO_2 there is a range of about 6 eV between the bottom of the conduction band to the next highest portion of the band (E_{intra}), in the α-PbO_2 that range is only about 4.7 eV. Thus, according to what has been discussed for Walsh et al.[3] it should be easier to manipulate the transparency in α-PbO_2 (controlling the oxygen vacancies or doping, for instance), thanks to move the electron chemical potential inside the conduction band, than to β-PbO_2. As it can be seen in the graphic, the theoretical valence band width is roughly 8.75 eV. Theoretical values reported for β-PbO_2 are 8.02 eV and 8.45 eV, depending on the functional used.[4] The conduction band shows a partition into two distinct regions separated by about 3 eV, which will be commented below when discussing the features of the density of states.

Total DOS profile and the most relevant projected DOS (PDOS) for Pb and O atoms are depicted in Figure 3. Following the notation adopted by Payne et al for β-PbO_2,[7] it has been identified three main features (labeled *I* - *III*) in the valence states of the total DOS profile. Region *III* is basically composed by a mix of 50% Pb 6s and 50% O 2p orbitals,

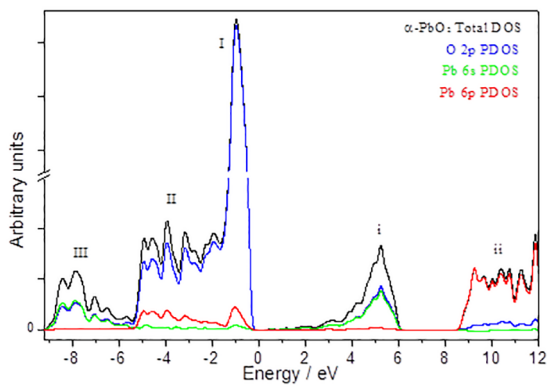

Figure 3. Total and partial DOS diagram for α-PbO_2.

showing that the states of lower energy are predominantly occupied for electrons equally distributed for those orbitals (it is usual to speak in terms of orbital hybridization). Region *II* is predominantly composed by oxygen 2p orbitals, with a residual contribution of the lead 6p orbitals, while in the highest energy band closest to the Fermi surface (region *I*), the contribution of lead 6p orbitals is, proportionally, even smaller, indicating a strong asymmetry in the electron distribution among the atoms. Thus, the energy states near the top of the valence band are predominantly occupied for electrons located in oxygen 2p orbitals. It deserves to pay attention that in the case of PbO_2, both lead 6s and 6p orbitals are, stoichiometric speaking, empty. Thus, it is understandable there are significant differences between the DOS distribution of this material and PbO, as it has been found, for example, by Watson and Parker.[52]

On the other hand, the conduction band shows two well defined regions, being that the empty states in the bottom (region *i*) are composed by equal contributions of O 2p and Pb 6s orbitals, while the states at higher energy (region *ii*) are predominantly composed of Pb 6p orbitals. It is remarkable the partition of the conduction band states into two distinct regions separated by a range of about 3 eV. Clearly this separation is related to that seen in the band structure profile, which has been highlighted above.

For a deeper comprehension of the electronic distribution throughout the material it has been plotted maps of electronic density distribution for some planes of α-PbO_2 (Figure 4). Some other planes have also been investigated, presenting the same profile. As a general behavior, it is noticed that the density isolines profiles show a well-defined charge distribution around the Pb and O atoms, an indication of the ionic character of the atomic interactions, accordingly to analysis done above. Thus, there is an asymmetry on the charge distribution through the material depending on the crystal direction. Aiming to detail further these founds it has been calculated the Pb - O overlap populations, which results are listed in the Table 2 (see unit cell shown in Figure 1 for atom numbering). Firstly, the values of the overlap population are about of that obtained for other studied oxide, ZnO (143 m|e|),[53] while the C - C overlap population of carbon nanotubes, a typical covalent bond is bigger than 400 m|e|.[53]

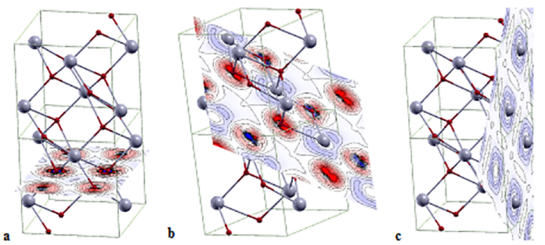

Figure 4. Charge density maps for 3 different α-PbO_2 planes (red denotes an excess of negative charge and blue a deficiency of it). **a**: oxygen only; **b**: oxygen and lead; **c**: lead only.

Table 2. Average Pb–O bond length (Å) and overlap population (m|e|) of α-PbO_2

	Pb1	Pb2
O1	2.123 (126)	-
O2	2.503 (58)	-
O3	2.137 (122)	-
O4	2.123 (126)	2.137 (122)
O5	-	2.441 (63)
O6	-	2.137 (122)

This result corroborates that Pb - O bond in α-PbO_2 has a ionic character. Secondly, there is a distinct difference among three of the oxygens (O1, O3 and O4) and O2 concerning to the Pb1 - O bond. The same behavior is observed also in the Pb - O bonds evolving Pb2, namely, the O2 - Pb1 and O5 - Pb2 bonds present a character yet slightly more ionic than the other bonds studied. This result is directly related to the bond lengths, shorter than the other Pb - O bonds, leading to an different charge distribution in each case.

Finally, the partial charges on the atoms calculated using Mulliken population analysis results -0.95 for oxygen and 1.90 for lead, yet indicating a predominate ionic character of the bonds. Obviously, these results should be viewed with caution, since the choice of Mulliken partition is arbitrary and the results depend on the basis set used. Besides, there is no unique method of performing the partition of the charge density. Even so, the choice of a particular scheme is still useful to support an argument.

4. Concluding Remarks

Electronic structure of α-PbO_2 has been studied by periodic DFT calculations. α-PbO_2 presented a theoretical band gap of 0.90 eV. The topography of the band structure suggests that transparency and conductivity can be achieved. Significant population of states at the top of the valence band arises from oxygen 2p states. The empty states are virtually composed of lead 6p and 6s, with a predominance of 6p orbitals. Maps of charge density for several planes shown that the material is predominantly ionic, which is confirmed by the overlap populations analysis. The charge distribution throughout the material depends on the crystal direction. Taking into account all these aspects, it may be expected a better suitability of α-PbO_2 to be applied as TCO than β-PbO_2. Several experimental techniques should be able of confirm these theoretical founds. The methodology used in the present case has also been used for studies of surfaces, doping and adsorption process, for example, and that will be the next goal in the investigation of the properties of both PbO_2 phases. The results obtained could suggest new properties and functionalities of these materials.

5. Acknowledgments

This work is supported by Brazilian Funding Agencies: CNPq (46126-4), CAPES (787027/2013, 8881.068492/2014-01), FAPESP (2013/07296-2, 2016/07476-9). The computational facilities were supported by resources supplied by Molecular Simulations Laboratory, São Paulo State University, Bauru, Brazil, and Laboratory of Computational Chemistry, São Paulo State University, Ilha Solteira, Brazil. JMMC is deeply grateful to Dr. Armando Beltrán, from University Jaume I, Castellon de la Plana, Spain, for his kind and fruitful discussions.

6. References

1. Berry JJ, Ginley DS, Burrows PE. Organic light emitting diodes using a Ga:ZnO anode. *Applied Physics Letters*. 2005;92(19):193304.
2. Fortunato E, Ginley D, Hosono H, Paine DC. Transparent Conducting Oxides for Photovoltaics. *MRS Bulletin*. 2007;32(3):242-247.
3. Walsh A, Kehoe AB, Temple DJ, Watson GW, Scanlon DO. PbO_2: from semi-metal to transparent conducting oxide by defect chemistry control. *Chemical Communications*. 2013;49(5):448-450.
4. Scanlon DO, Kehoe AB, Watson GW, Jones MO, David WIF, Payne DJ, et al. Nature of the Band Gap and Origin of the Conductivity of PbO_2 Revealed by Theory and Experiment. *Physical Review Letters*. 2011;107(24):246402.
5. Rothenberg S, Payne DJ, Bourlange A, Egdell RG. A study of the metal to nonmetal transition in Bi-doped β-PbO_2 by high resolution x-ray photoemission. *Journal of Applied Physics*. 2007;102(11):113717.
6. Payne DJ, Egdell RG, Paolicelli G, Offi F, Panaccione G, Lacovig P, et al. Nature of electronic states at the Fermi level of metallic β-PbO_2 revealed by hard x-ray photoemission spectroscopy. *Physical Review B*. 2007;75(15):153102.
7. Payne DJ, Egdell RG, Law DSL, Glans PA, Learmonth T, Smith KE, et al. Experimental and theoretical study of the electronic structures of α-PbO and β-PbO_2. *Journal of Materials Chemistry*. 2007;17:267-277.
8. Payne DJ, Egdell RG, Hao W, Foord JS, Walsh A, Watson GW. Why is lead dioxide metallic? *Chemical Physics Letters*. 2005;411(1-3):181-185.
9. Costa FR, Silva JM. Factors governing the formation of the β-PbO_2 phase electroformed galvanostatically on the carbon cloth substrate. *Química Nova*. 2012;35(5):962-967.
10. D'Alkaine CV, Cordeiro JMM. Active-passive transition of lead in sulfuric acid solutions. in: Bullock KR, Pavlov D, eds. *Advances in Lead Acid Batteries, Electrochemical Society Proceedings*. Pennigton: Electrochemical Society; 1984. p. 190-200.
11. Chopra KL, Major S, Pandya DK. Transparent conductors - A status review. *Thin Solid Films*. 1983;102(8):1-46.

12. Payne DJ, Paolicelli G, Offi F, Panaccione G, Lacovig P, Beamson G, et al. A study of core and valence levels in β-PbO_2 by hard X-ray photoemission. *Journal of Electron Spectroscopy and Related Phenomena*. 2009;169(1):26-34.

13. Burbano M, Scanlon DO, Watson GW. Sources of Conductivity and Doping Limits in CdO from Hybrid Density Functional Theory. *Journal of the American Chemical Society*. 2011;133(38):15065-15072.

14. Yang Y, Jin S, Medvedeva JE, Ireland JR, Metz AW, Ni J, et al. CdO as the Archetypical Transparent Conducting Oxide. Systematics of Dopant Ionic Radius and Electronic Structure Effects on Charge Transport and Band Structure. *Journal of the American Chemical Society*. 2005;127(24):8796-8804.

15. Moss TS. The Interpretation of the Properties of Indium Antimonide. *Proceedings of the Physical Society. Section B*. 1954:67(10):775-782.

16. Burstein E. Anomalous Optical Absorption Limit in InSb. *Physical Review*. 1954;93(3):632-633.

17. Kíliç C, Zunger A. Origins of coexistence of conductivity and transparency in SnO_2. *Physical Review Letters*. 2002;88(9):095501.

18. Segev D, Wei SH. Structure-derived electronic and optical properties of transparent conducting oxides. *Physical Review B*. 2005;71(12):125129.

19. Dovesi RS, Saunders VR, Roetti C, Orlando R, Zicovich-Wilson CM, Pascale F, et al. *CRYSTAL14 User's Manual*. Turin: University of Torino; 2014.

20. Maul J, Erba A, Santos IMG, Sambrano JR, Dovesi R. In silico infrared and Raman spectroscopy under pressure: the case of $CaSnO_3$ perovskite. *Journal of Chemical Physics*. 2015;142(1):014505.

21. Albuquerque AR, Bruix A, Sambrano JR, Illas F. Theoretical Study of the Stoichiometric and reduced Ce-doped TiO_2 anatase (001) surfaces. *Journal of Physical Chemistry C*. 2015;119(9):4805-4816.

22. Lejaeghere K, Bihlmayer G, Björkman T, Blaha P, Blügel S, Blum V, et al. Reproducibility in density functional theory calculations of solids. *Science*. 2016;351(6280):aad3000. DOI: 10.1126/science.aad3000

23. Souza SF, Fernandes PA, Ramos MJ. General Performance of Density Functionals. *Journal of Physical Chemistry A*. 2007;111(42):10439-10452.

24. Pisani C, Dovesi R, Roetti C. *Hartree-Fock Ab Initio Treatment of Crystalline Systems*. Berlin Heidelberg: Springer-Verlag; 1988.

25. Becke AD. Density-functional thermochemistry. III. The role of exact exchange. *Journal of Chemical Physics*. 1993;98(7):5648-5652.

26. Lee C, Yang W, Parr GR. Development of the Colle-Salvetti correlation-energy formula into a functional of the electron density. *Physical Review B*. 1988;37(2):785-789.

27. Heyd J, Scuseria GE, Ernzerhof M. Hybrid functionals based on a screened Coulomb potential. *Journal of Chemical Physics*. 2003;118(18):8207-8215.

28. Tirado-Rives J, Jorgensen WL. Performance of B3LYP Density Functional Methods for a Large Set of Organic Molecules. *Journal of Chemical Theory and Computation*. 2008;4(2):297-306.

29. Perdew JP, Ernzerhof M, Burke K. Rationale for mixing exact exchange with density functional approximations. *Journal of Chemical Physics*. 1996;105(22):9982-9985.

30. Ernzerhof M, Perdew JP, Burke K. Coupling-constant dependence of atomization energies. *International Journal of Quantum Chemistry*. 1997;64(3):285-295.

31. Ernzerhof M, Scuseria GE. Assessment of the Perdew-Burke-Ernzerhof exchange-correlation functional. *Journal of Chemical Physics*. 1999;110(11):5029-5036.

32. Grimme S. Accurate description of van der Waals complexes by density functional theory including empirical corrections. *Journal of Computational Chemistry*. 2004;25(12):1463-1473.

33. Grimme S. Semiempirical GGA-type density functional constructed with a long-range dispersion correction. *Journal of Computational Chemistry*. 2006;27(15):1787-1799.

34. Albuquerque AR, Garzim ML, Santos IMG, Longo V, Longo E, Sambrano JR. DFT Study with Inclusion of the Grimme Potential on Anatase TiO_2: Structure, Electronic, and Vibrational Analyses. *Journal of Physical Chemistry A*. 2012;116(47):11731-11735.

35. Civalleri B, Zicovich-Wilson CM, Valenzano L, Ugliengo P. B3LYP augmented with an empirical dispersion term (B3LYP-D*) as applied to molecular crystals. *CrystEngComm*. 2008;10(4):405-410.

36. Canepa P, Ugliengo P, Alfredsson M. Elastic and Vibrational Properties of α- and β-PbO. *Journal of Physical Chemistry C*. 2012;116(40):21514-21522.

37. Monkhorst HJ, Pack JD. Special points for Brillouin-zone integrations. *Physical Review B*. 1976;13(2):5188-5192.

38. Kokalj A. XCrySDen-a new program for displaying crystalline structures and electron densities. *Journal of Molecular Graphics and Modelling*. 1999;17(3-4):176-179.

39. Gatti C, Saunders VR, Roetti C. Crystal field effects on the topological properties of the electron density in molecular crystals: The case of urea. *Journal of Chemical Physics*. 1994;101(12):10686-10696.

40. Peintinger MF, Oliveira DV, Bredow T. Consistent Gaussian basis sets of triple-zeta valence with polarization quality for solid-state calculations. *Journal of Computational Chemistry*. 2013;34(6):451-459.

41. Nizam M, Bouteiller Y, Silvi B, Pisani C, Causa M, Dovesi R. A theoretical investigation of electronic structure and some thermodynamical properties of β-PbF_2. *Journal of Physics C: Solid State Physics*. 1988;21(31):5351-5359.

42. Piskunov S, Heifets E, Eglitis RI, Borstel G. Bulk properties and electronic structure of $SrTiO_3$, $BaTiO_3$, $PbTiO_3$ perovskites: an ab initio HF/DFT study. *Computational Materials Science*. 2004;29(2):165-178.

43. Sophia G, Baranek P, Sarrazin C, Rérat M, Dovesi R. First-principles study of the mechanisms of the pressure-induced dielectric anomalies in ferroelectric perovskites. *Phase Transitions*. 2013;86(11):1069-1084.

44. Cordeiro JMM, Soper AK. A hybrid neutron diffraction and computer simulation study on the solvation of N-methylformamide in dimethylsulfoxide. *Journal of Chemical Physics*. 2013;138(4):044502.

45. Borges A, Cordeiro JMM. Hydrogen bonding donation of N-methylformamide with dimethylsulfoxide and water. *Chemical Physics Letters*. 2013;565:40-44.

46. Cordeiro JMM, Soper AK. Investigation on the structure of liquid N-methylformamide-dimethylsulfoxide mixtures. *Chemical Physics*. 2011;381(1-3):21-28.

47. Almeida GG, Cordeiro JMM. A Monte Carlo revisiting of N-methylformamide and acetone. *Journal of the Brazilian Chemical Society*. 2011;22(11):2178-2185.

48. Moura KF, Maul J, Albuquerque AR, Casali GP, Longo E, Keyson D, et al. TiO_2 synthesized by microwave assisted solvothermal method: Experimental and theoretical evaluation. *Journal of Solid State Chemistry*. 2014;210(1):171-177.

49. Floriano EA, Scalvi LVA, Saeki MJ, Sambrano JR. Preparation of TiO_2/SnO_2 Thin Films by Sol-Gel Method and Periodic B3LYP Simulations. *Journal of Physical Chemistry A*. 2014;118(31):5857-5865.

50. Ferrer MM, Santana YVB, Raubach CW, La Porta FA, Gouveia AF, Longo E, et al. Europium doped zinc sulfide: a correlation between experimental and theoretical calculations. *Journal of Molecular Modeling*. 2014;20:2375.

51. Miundat.org. Scrutinyite. Available from: <http://www.mindat.org/min-3598.html>. Access in: 02/01/2017.

52. Watson GW, Parker SC. Origin of the Lone Pair of α-PbO from Density Functional Theory Calculations. *Journal of Physical Chemistry B*. 1999;103(8):1258-1262.

53. Marana NL, Albuquerque AR, La Porta FA, Longo E, Sambrano JR. Periodic density functional theory study of structural and electronic properties of single-walled zinc oxide and carbon nanotubes. *Journal of Solid State Chemistry*. 2016;237:36-47.